A Single Light-Source Configuration for Full-Duplex 60-GHz-Band Radio-on-Fiber System

Toshiaki Kuri, *Member, IEEE*, Ken-ichi Kitayama, *Senior Member, IEEE*, and Yoshiro Takahashi

***Abstract*—A simple full-duplex radio-on-fiber system using a single light source is described. A base station (BS) is simplified by giving it no local light or RF sources. The optical carrier for the uplink is sent along with the downlink optical signal to a remote BS. It is looped back to the central station after being modulated with an uplink RF signal. Fiber-optic full-duplex transmission of 60-GHz-band 155.52-Mb/s downlink and uplink signals over 25-km-long standard single-mode fibers is experimentally demonstrated and bit error rates of 10^{-9} for both links were achieved without any serious fiber dispersion due to the optical single-sideband format. The configuration of the proposed system is simpler because one light source is shared by the downlink and uplinks.**

***Index Terms*—Chromatic fiber dispersion, electroabsorption modulator (EAM), full-duplex transmission, optical single sideband (SSB), radio-on-fiber system.**

I. Introduction

MILLIMETER-WAVE is a promising frequency resource for future broad-band radio communication systems [1], [2]. Radio-on-fiber systems are attracting a great deal of attention because it is transparent and flexible for RF signals [3], [4].

The key to making millimeter-wave radio-on-fiber systems practical for commercial deployment is developing a low-cost base station (BS). The external modulation technique is one of the best solutions in order to provide a simple system configuration [5]. We have demonstrated fiber-optic millimeter-wave downlink and uplink systems using a 60-GHz-band electroabsorption modulator (EAM) [6], [7]. The system configurations are illustrated in Fig. 1. In the uplink system [see Fig. 1(b)], 60-GHz-band photonic downconversion was performed by a remotely fed optical pilot tone [7]. Transmitting only two optical frequency components, which are one replica of the received millimeter-wave uplink signal ($f_c - f_u$) and the neighbor pilot tone ($f_c - f_l$), is enough to extract the uplink data through the IF signal ($f_u - f_l$), where f_c, f_u, and f_l are the central frequencies of optical carrier, millimeter-wave uplink signal, and millimeter-wave local tone, respectively. As a result, the received millimeter-wave signal (f_u) was converted to a microwave IF signal ($f_u - f_l$) not only without any millimeter-wave mixer, but also without any serious fiber-dispersion effect. The simple combination of the proposed downlink and uplink systems with the function of photonic downconversion will be a candidate of full-duplex systems; however, it uses two light sources and two optical modulators (EAM_{C1} and EAM_{C2}) in the central stations (CSs) in addition to the third EAM (EAM_B) at the BS. We consider this on the reduction of optical components and the sharing of optical resources. In [4], one of the full-duplex systems without a light source in the BS have been reported, which had the feature of the reuse of an optical carrier by making good use of some fiber Bragg gratings (FBGs). However, it has been difficult to perform the photonic downconversion because only the optical carrier was reused. In [8], another full-duplex system using a single light source and loop back configuration has been proposed, which transmitted an IF signal with an EAM transceiver.

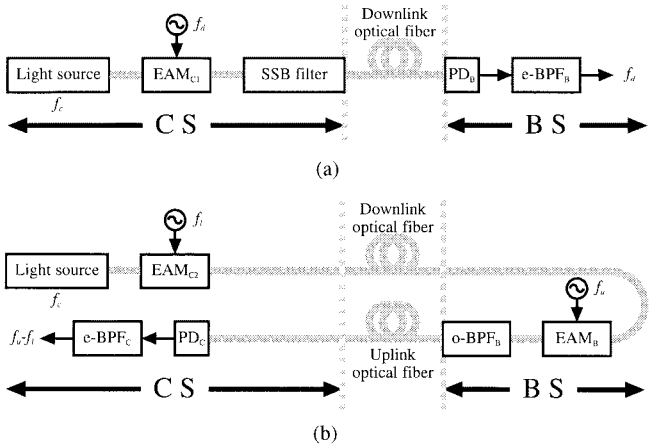

Fig. 1. Block diagrams of reported: (a) downlink and (b) uplink system.

In this paper, we further simplify the configuration of the full-duplex 60-GHz-band millimeter-wave radio-on-fiber system based on the external modulation technique [9]. The proposed system has the following advantages.

- First, it uses a single light source and a single optical modulator in the CS in spite of the full-duplex operation.
- Second, the BS is simplified by giving it no local light or RF sources. It is distinct from [8] in that no remote upconversion is performed for the downlink.
- Third, the optical downlink carrier is reused for the uplink. The signal is photodetected to generate the desired downlink RF signal, and a fraction of the signal is looped back to be used as the uplink optical carrier. It is distinct from [4] in that the photonic downconversion is performed for the uplink.

Manuscript received October 15, 2001; revised April 18, 2002. This paper was presented in part at the 1999 International Topical Meeting on Microwave Photonics (MWP'99), Melbourne, Australia, November 17–19, 1999.

T. Kuri is with the Basic and Advanced Research Division, Communications Research Laboratory, Tokyo 184-8795, Japan (e-mail: kuri@crl.go.jp).

K. Kitayama is with the Department of Electronics and Information Systems, Graduate School of Engineering, Osaka University, Osaka 565-0871, Japan.

Y. Takahashi is with the System Solutions Company, Oki Electric Industry Company Ltd., Kanagawa 239-0847, Japan.

Digital Object Identifier 10.1109/TMTT.2002.807837

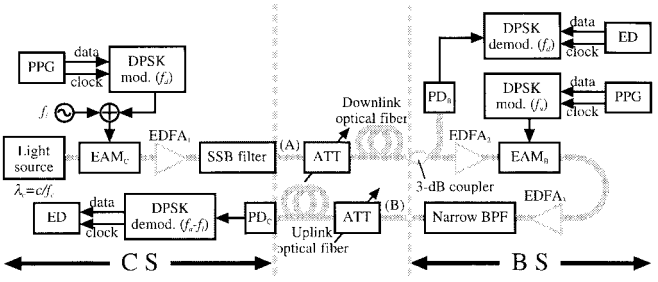

Fig. 2. Proposed system configuration.

- Finally, to overcome the fading of the photodetected signal due to the fiber dispersion effect [10], the optical single-sideband (SSB) format is used by suppressing the one sideband with optical filters for both links [6].

The principle of the proposed system is theoretically described. The simultaneous fiber-optic transmission of both 155.52-Mb/s differential phase-shift keying (DPSK) downlink and uplink signals on 60-GHz-band millimeter-wave carriers over 25-km-long standard single-mode fibers (SMFs) for each optical link is experimentally demonstrated. The proposed technique leads to a simple system configuration by sharing the light source for the downlink and uplinks. The theory and modification of the system configuration are the significant additions to [9].

II. System Descriptions

The proposed system configuration is shown in Fig. 2. The system basically consists of a light source, two optical external modulators (EAM_C and EAM_B), two photodetectors (PD_C and PD_B), an optical SSB filter, an optical power divider (3-dB coupler), an optical narrow bandpass filter (BPF), two DPSK modulators (mods.), and two electrical BPFs, which are included in each DPSK demodulators (demods.). The electrical BPFs were used to eliminate the unwanted frequency components. Here, they will be required even in actual systems because of the radio regulation. No local light or RF sources for transmission is located at the BS. The CS and BS are connected by downlink and uplink standard SMFs. The detailed principle is described in the Appendix.

A. Downlink

First, an optical carrier with the wavelength λ_c (frequency $f_c = c/\lambda_c$, where c is the optical velocity in vacuum) from the light source is simultaneously modulated with an RF downlink signal with frequency f_d and an RF local tone with frequency f_l by EAM_C in the CS. To overcome the fiber dispersion effect, upper sidebands (USBs) ($f_c + f_l$ and $f_c + f_d$) are eliminated by the optical SSB filter [6]. Hence, the carrier (f_c) and lower sidebands (LSBs) ($f_c - f_l$ and $f_c - f_d$) are transmitted to the remote BS, as shown in Fig. 3(a). The transmitted optical signal is expressed as follows:

$$e_{\mathrm{down}}(t) \propto a_{-1,0}\cdot e^{j\{2\pi(f_c-f_d)t-\theta_d(t)+\phi_c(t)\}} + a_{0,-1}\cdot e^{j\{2\pi(f_c-f_l)t+\phi_c(t)\}} + a_{0,0}\cdot e^{j2\pi f_c t+\phi_c(t)}. \quad (1)$$

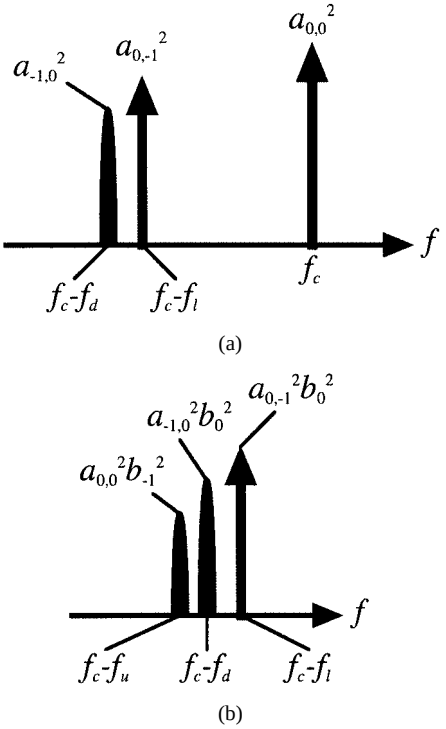

Fig. 3. Optical spectra of: (a) downlink and (b) uplink signal.

$a_{-1,0}$, $a_{0,-1}$, and $a_{0,0}$ represent the relative amplitudes of downlink, local tone, and carrier components, respectively, which are decided by optical modulation format [7]. $\theta_d(t)$ and $\phi_c(t)$ are the downlink data and the laser phase noise, respectively. Part of the transmitted optical signal (called an optical downlink signal) is tapped by the optical power divider and photodetected to regenerate the RF downlink signal (f_d) at PD_B in the BS. Undesired RF local tone (f_l) must be far enough away from the desired RF signal (f_d) to be easily eliminated by the electrical BPF in the BS. As shown in Section III, it was achieved if they had 3-GHz spacing. The desired RF signal after transmitting over the L_d-long downlink SMF is expressed by (see the Appendix)

$$i_{\mathrm{down}}(t, L_d) \propto a_{0,0}a_{-1,0}\cdot e^{j\varphi_{c,d}(t,L_d)} \quad (2)$$

$$\varphi_{c,d}(t, L_d) = 2\pi f_d(t-\beta_{d1}L_d) + \theta_d(t-\beta_{d1}L_d) - \frac{1}{2}\beta_{d2}(2\pi f_d)^2 L_d \quad (3)$$

where $\beta_{d1}L_d$ corresponds to the group-delay time, and β_{d2} is related with the dispersion of downlink fiber D_d as [13]

$$\beta_{d2} = -\frac{\lambda^2}{2\pi c}\cdot D_d. \quad (4)$$

λ is the wavelength in the fiber. Note that, in (3), the last term is a constant phase, and there is no laser phase noise term. If the payload data of the RF downlink signal $\theta_d(t)$ is differentially encoded and then the propagating RF downlink signal $i_{\mathrm{down}}(t, L_d)$ is demodulated by the differential detection, the data for the downlink can be extracted without any fiber dispersion effect, as well as no laser phase noise. Our technique could be also used with multilevel phase-shift keying (PSK) modulation schemes with differential-encoding data.

B. Uplink

A fraction of the optical signal transmitted from the CS is again modulated with an RF uplink signal (f_u) at the BS. By this modulation, a number of frequency components in the optical frequency domain are generated, including some replicas of data on the RF uplink signal. After optical bandpass filtering at the BS, only the optical uplink signal is transmitted to the CS, as shown in Fig. 3(b). The optical uplink signal is expressed as

$$e_{\mathrm{up}}(t, L_d) \propto a_{-1,0}\cdot b_0\cdot e^{j\psi_{-1,0}(t, L_d)} + a_{0,-1}\cdot b_0\cdot e^{j\psi_{0,-1}(t, L_d)} + a_{0,0}\cdot b_{-1}\cdot e^{j\{\psi_{0,0}(t, L_d)-2\pi f_u t-\theta_u(t)\}} \quad (5)$$

where $\theta_u(t)$ is the payload data of the uplink signal and $\psi_{p,q}(t, L_d)$ is defined as

$$\begin{aligned}\psi_{p,q}(t, L_d) =& 2\pi(f_c + pf_d + qf_l)(t-\beta_{d1}L_d) \\ &+ \phi_c(t-\beta_{d1}L_d) + p\theta_d(t-\beta_{d1}L_d) \\ &- \frac{1}{2}\beta_{d2}\cdot\{2\pi(pf_d+qf_l)\}^2\cdot L_d \\ &- (\beta_{d0}-\beta_{d1}\cdot 2\pi f_c)\cdot L_d. \end{aligned} \quad (6)$$

The optical uplink signal looped back is photodetected to generate the desired IF signal ($f_u - f_l$) by photonic down-conversion [7]. The photonic-downconverted IF signal after transmitting over the L_u-long uplink SMF is expressed as follows (see the Appendix):

$$i_{\mathrm{up}}(t, L_d, L_u) \propto a_{0,0}a_{0,-1}b_0b_{-1}\cdot e^{j\varphi_{l,u}(t, L_d, L_u)} \quad (7)$$

$$\begin{aligned}\varphi_{l,u}(t, L_d, L_u) =& 2\pi(f_u-f_l)(t-\beta_{d1}L_d-\beta_{u1}L_u) \\ &+ \theta_u(t-\beta_{u1}L_u) - \frac{1}{2}\beta_{d2}(2\pi f_l)^2L_d \\ &- \frac{1}{2}\beta_{u2}(2\pi f_l)^2L_u + \frac{1}{2}\beta_{u2}(2\pi f_u)^2L_u \\ &+ \beta_{d1}(2\pi f_u)L_d. \end{aligned} \quad (8)$$

Here, $\beta_{u1}L_u$ corresponds to the group-delay time and β_{u2} is related with the dispersion of downlink fiber D_u as [13]

$$\beta_{u2} = -\frac{\lambda^2}{2\pi c}\cdot D_u. \quad (9)$$

Note that, in (8), the last four terms are constant phases, and there is no laser phase noise term. If the payload data of the RF uplink signal $\theta_u(t)$ is deferentially encoded and then the down-converted IF downlink signal $i_{\mathrm{up}}(t, L_d, L_u)$ is demodulated by the differential detection, the data for the uplink can be also extracted without any fiber dispersion effect, as well as no laser phase noise.

III. Experiment

A. Experimental Setup

Experiments were performed by using the setup shown in Fig. 2. The optical system in the CS consisted of a distributed-feedback laser diode (DFB LD) as the light source, EAM_C as an Erbium-doped fiber amplifier (EDFA_1), an optical SSB filter, and PD_C. Those in the BS consisted of two EDFAs (EDFA_2 and EDFA_3), a 3-dB directional optical coupler, PD_B, EAM_B, and an optical narrow BPF. The CS and BS were linked by two 25-km-long uplink and downlink SMFs. Optical attenuators (ATTs) in front of the SMFs were used in order to control the transmitting optical powers. The EAM_C and EAM_B modules were packaged with input and output fibers [6], [7]. The EAM_C and EAM_B modules were packaged with input and output fibers and were designed to have the 15-dB return loss of approximately 3 GHz centered at 60 GHz [6], [7]. The polarization dependencies of EAM_C and EAM_B were designed to be less than 0.5 dB. Therefore, no polarization control was performed. Wide-band PDs with the 3-dB bandwidth of 10 and 50 GHz were used as the PD_C and PD_B. The optical SSB filter consisted of a Fabry–Perot etalon filter and an optical BPF with 3-dB bandwidth of 0.5 nm [6]. This could be replaced with an FBG as a notch filter [12].

In the CS, an optical carrier ($\lambda_c = 1553.9$ nm) was intensity modulated by EAM_C with a subcarrier multiplexed signal composed of a 59.064-GHz ($=f_d$) DPSK signal with a data rate of 155.52 Mb/s and a 57.000-GHz ($=f_l$) sinusoidal wave from a synthesized continuous wave (CW) generator (Anritsu 69097B). Downlink data of 155.52 Mb/s was generated by a pulse-pattern generator (PPG) (Anritsu MP163220A) with a pseudorandom bit sequence (PRBS) of $2^{23}-1$. The bias of EAM_C was -1.6 V, optimized to achieve the lowest bit error rate (BER). The total optical insertion loss of the module was approximately 13 dB at this bias. The modulated optical signal was amplified by EDFA_1, filtered by the optical SSB filter, which allowed only both the carrier and first-order LSB to pass, and then transmitted to the remote BS over the 25-km-long downlink SMF. The optical SSB filtering prevents signal fading due to fiber dispersion after photodetection. The downlink data is on the optical component at $f_c - f_d$ in Fig. 3(a).

After being in the BS, half of the optical downlink signal was photodetected to regenerate the 59.064-GHz downlink signal, and then the data and clock were extracted by a DPSK demodulator (demod.) at f_d. In the DPSK demodulator, the Butterworth filter with a 3-dB bandwidth of 234 MHz was included to eliminate the undesired local tone photodetected from the optical component at $f_c - f_l$. The BER was measured from the extracted downlink data with an error detector (ED) (Anritsu MP163240A).

The fraction of the optical downlink signal was amplified by EDFA_2 and again intensity modulated with the 60.000-GHz uplink signal with a data rate of 155.52 Mb/s by EAM_B. The modulated signal was again amplified by EDFA_3 to compensate for the insertion losses of EAM_B, the following narrow BPF, and the 25-km-long uplink SMF. The uplink data with a rate of 155.52 Mb/s was generated by another PPG (Anritsu MP1650A) with a PRBS of $2^{23}-1$. The optimized bias of EAM_B was -1.8 V. The total optical insertion loss of the module was approximately 11 dB at a bias of -1.8 V. To construct the narrow BPF, we used two arrayed waveguide gratings (AWGs), each with a frequency interval of 0.48 nm (60 GHz at 1.55 μm), a full-width at half maximum (FWHM) of 0.19 nm, an insertion loss of less than 4.3 dB, crosstalk of less then -30 dB, and a reflection loss of less then -50 dB [11]. Here, FBGs may also be a candidate of narrow BPFs to reduce the insertion loss instead of AWGs [4], [14].

The uplink optical signal that was looped back to the CS was photodetected by PD_C to generate the desired IF signal at $f_u -$

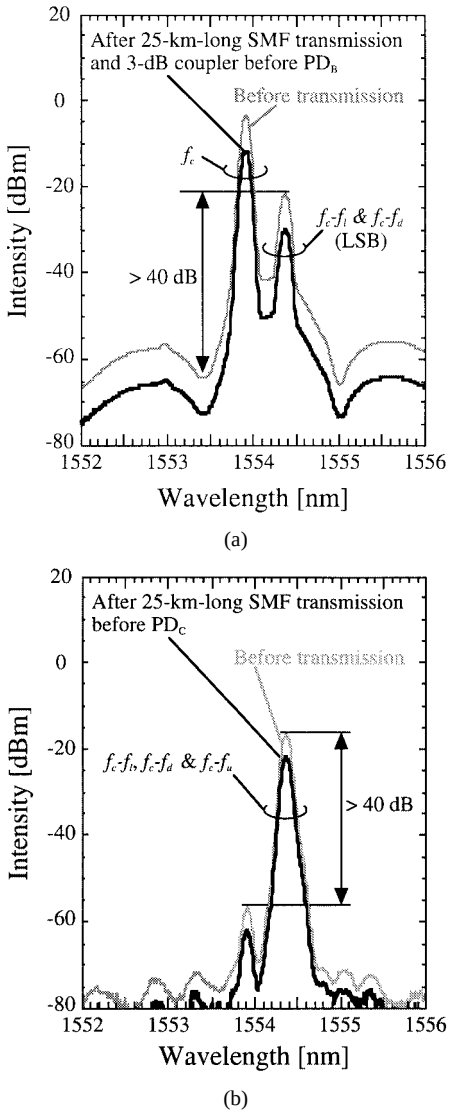

Fig. 4. Measured optical spectra. (a) Downlink signal. (b) Uplink signal.

f_l (= 3.000 GHz). The DPSK demodulator at $f_u - f_l$ in the CS also had a Butterworth filter with a 3-dB bandwidth of 234 MHz and eliminated the undesired signals ($f_d - f_l$ and $f_u - f_d$) before extracting the data and clock. The BER of the extracted uplink data was measured with another ED (Anritsu MP1651A).

B. Experimental Results and Discussion

Spectra of optical downlink and uplink signals were measured. They are shown in Fig. 4. The USB in the optical downlink signal was suppressed by over 40 dB by the optical SSB filter [see Fig. 4(a)] [6]. After the 25-km-long downlink SMF transmission and passing through the 3-dB coupler, the optical loss was 8 dB due to the 5-dB transmission loss of the 25-km-long uplink SMF (0.2 dB/km) and due to the 3-dB coupler, as theoretically predicted. The optical loss of 5 dB for the uplink was also due to the 25-km-long uplink SMF, as shown in Fig. 4(b).

The measured spectra of the photodetected RF downlink and IF uplink signals are shown in Fig. 5. Both signals were modulated without any data. The photodetected signals were generated without any serious interchannel interference. No serious

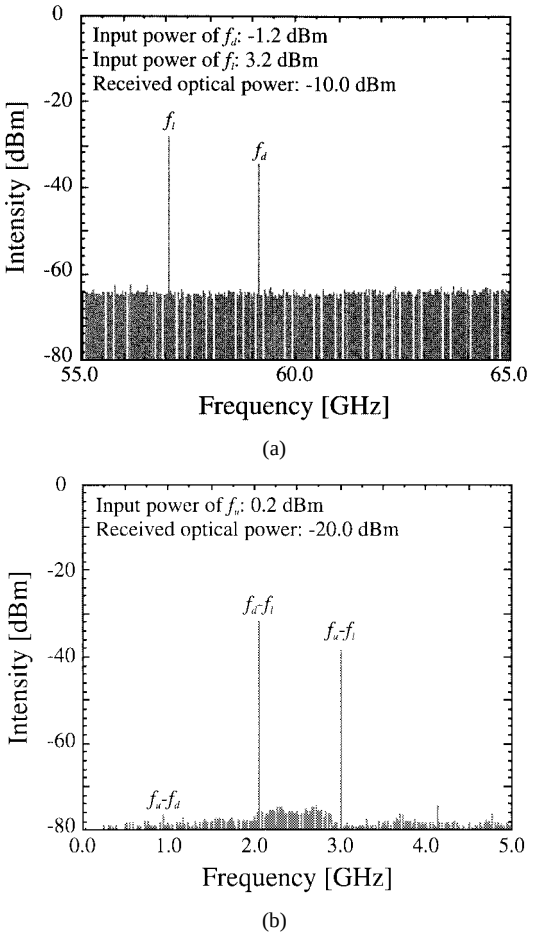

Fig. 5. Spectra of photodetected signals after 25-km-long SMF transmission: (a) at PD_B in the BS and (b) at PD_C in the CS.

intermodulation distortion was observed either due to the small modulation depths. Since the frequency difference between the desired and undesired signals was 936 MHz ($\simeq 155.52 \times 6$), the undesired spectra at f_l in Fig. 5(a) and at $f_d - f_l$ and $f_u - f_d$ in Fig. 5(b) can be easily eliminated by the following electrical BPF in each DPSK demodulator.

The data for the downlink and uplinks were simultaneously transmitted. Fig. 6 shows the BER after the 25-km-long downlink and uplink SMF transmissions and the back-to-back. The RF powers put into the EAMs of f_l, f_d, and f_u were, again, 3.2, -1.2, and 0.3 dBm, respectively. The optical powers put into EAM_C and EAM_B were 2.2 and 3.0 dBm, respectively. No BER floor or power penalty was observed for either link. After the 25-km-long SMF transmission, the minimum received optical power to simultaneously achieve a BER of 10^{-9} was -13 and -24 dBm for the downlink and uplinks, respectively. Since optical SSB signal transmission is performed for both links, this system is essentially free from the fiber-dispersion effect within 25-km-long SMF transmission.

The BERs as a function of the RF powers put into EAM_C and EAM_B for the downlink and uplinks are also plotted in Fig. 7. The optical power received by PD_B and PD_C was -10 and -20 dBm, respectively. Again, no BER floor was observed within the measured range of RF power. The minimum RF input power to simultaneously achieve a BER of 10^{-9} was -6 and -3 dBm for the downlink and uplinks, respectively.

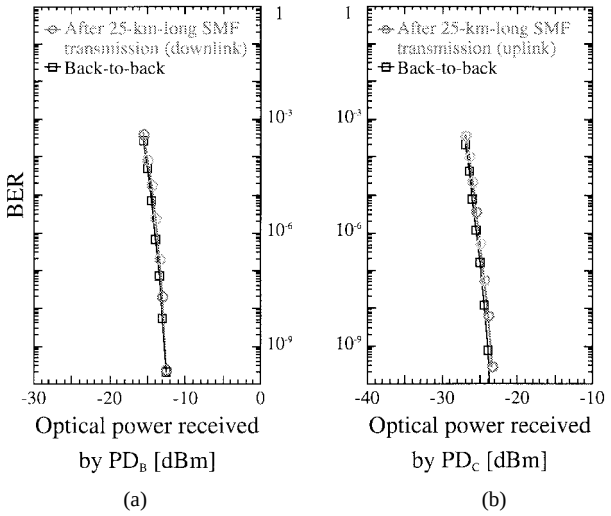

Fig. 6. BER versus optical power received by the PD. RF input power was: (a) −1.2 dBm for the downlink and (b) 0.3 dBm for the uplink.

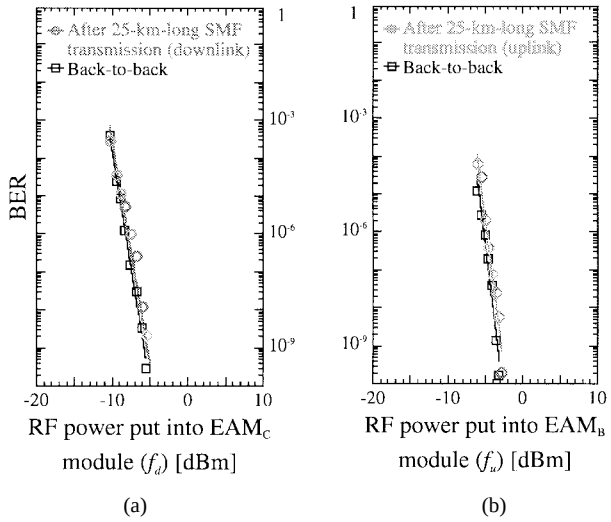

Fig. 7. BER versus RF input power. Optical power received was: (a) −10 dBm for the downlink and (b) −20 dBm for the uplink.

The optical sensitivity, which is defined as the minimum optical received power needed to achieve a BER of 10^{-9}, was measured as a function of the RF power put into the EAM module for the downlink and uplinks. The results are plotted in Fig. 8(a). The sensitivity for the downlink was proportional to the RF power put into EAM_C within the measured range. The sensitivity for the uplink was proportional to the input RF power put into EAM_C at more than −2 dBm, but became levels off below −3 dBm. The difference of sensitivity for both links was also observed in the unsaturated region. It is considered that the penalty was mainly caused by amplified spontaneous emission (ASE) noise from EDFA_2 and EDFA_3, where the total noise figure of the EDFAs is estimated to be approximately 9 dB at 0-dBm RF input.

The modulation depth and signal-to-noise power ratio (SNR) of the LSB component of the optical uplink signal were also measured. The results are plotted as a function of the uplink RF

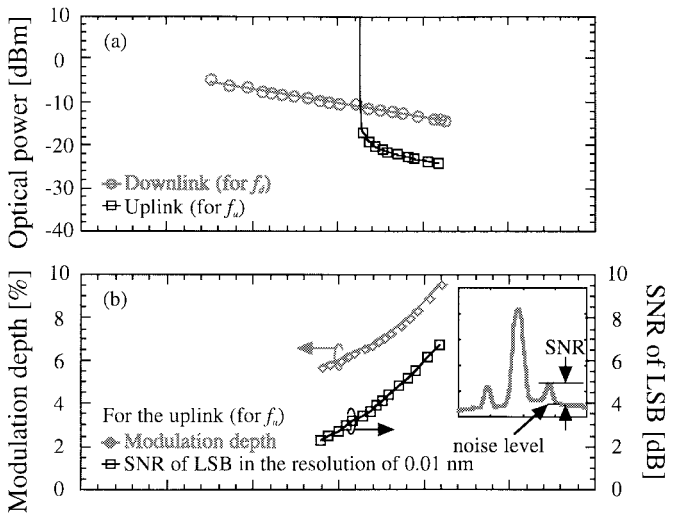

Fig. 8. (a) Optical sensitivity to achieve the BER of 10^{-9}. Power of RF local tone was 3.2 dBm. (b) Estimated modulation depth and SNR of LSB for uplink.

power into EAM_B in Fig. 8(b). The SNR is defined as shown in the inset of Fig. 8(b). The resolution of an optical spectrum analyzer was 0.01 nm. The modulation depth increased as the uplink RF input power increased. Since the ASE noise level was almost constant within the measured range, the SNR decreased as the modulation depth decreased. We can see that, in order to achieve the BER of 10^{-9}, the SNR of over 3.5 dB in 0.01-nm resolution is necessary.

In the experiment, the optical power margins for both links were 7–11 dB due to the optical ATTs, even for 25-km-long fiber-optic transmission. Therefore, some or all of the EDFAs used could be removed if the received optical power was large enough to achieve a BER of 10^{-9}. If, for example, one of the EDFAs that was used for power compensation in the experiment can be removed, the SNR of the LSB will be improved by 3 dB at least because an ideal noise figure of EDFA is 3 dB. As a result, the minimum RF power to be applied to the EAM for the uplink could be reduced to −6 dBm.

IV. Conclusion

A full-duplex 60-GHz-band millimeter-wave radio-on-fiber system using a single light source has been described. This system has had fewer optical components than conventional systems because its configuration is simpler due to the BS having no local light or RF sources. The additional optical amplifiers to compensate for the insertion losses will be shared effectively in future wavelength division multiplexing (WDM) systems. Since the optical downlink and uplink signals are in an optical SSB format, there has been no serious dispersion problem. BERs of less than 10^{-9} have been simultaneously achieved for fiber-optic transmission of 60-GHz-band, 155.52-Mb/s DPSK downlink, and uplink signals over 25-km-long SMFs.

Optical sensitivity can become saturated in the uplink, but optimizing the EDFA drive condition should alleviate this problem.

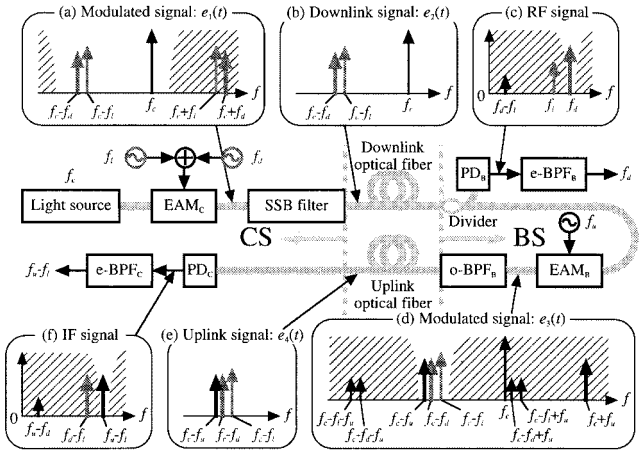

Fig. 9. Fundamental system configuration and frequency allocations.

APPENDIX
GENERAL MATHEMATICAL DESCRIPTIONS FOR DOWNLINK AND UPLINK SIGNALS

Fig. 9 shows the fundamental configuration and frequency allocations of the proposed system. In the radio-on-fiber system, only the fundamental and first-order sidebands are of interest, as shown in Fig. 9. For simplicity, optical power loss or gain in each optical component are omitted below.

An optical carrier with the constant power of P_c, carrier frequency of f_c, and phase noise of $\phi_c(t)$ from a single-mode light source is generated from a single-mode light source. The complex electric field of optical carrier $e_c(t)$ is usually expressed by

$$e_c(t) \propto \sqrt{2P_c}\exp\{j\varphi_c(t)\} \tag{A1}$$
$$\varphi_c(t) = 2\pi f_c t + \phi_c(t). \tag{A2}$$

An optical modulator (MOD_C) modulates the optical carrier $e_c(t)$ with a combined signal of an RF downlink signal $m_d(t)$ and an RF local tone $m_l(t)$

$$m_d(t) = V_d \cdot \exp\{j\varphi_d(t)\} \tag{A3}$$
$$m_l(t) = V_l \cdot \exp\{j\varphi_l(t)\} \tag{A4}$$
$$\varphi_d(t) = 2\pi f_d t + \theta_d(t) \tag{A5}$$
$$\varphi_l(t) = 2\pi f_l t. \tag{A6}$$

V_d, f_d, and $\theta_d(t)$ are the amplitude, carrier frequency, and payload data of the RF downlink signal, respectively. V_l and f_l are the amplitude and carrier frequency of the RF local tone, respectively. For the subcarrier modulation, the complex electric field of the modulated optical signal $e_1(t)$ is, in general, written as

$$e_1(t) = \mathbf{M}_C\big[m_d(t) + m_l(t)\big]\cdot e_c(t) = \sqrt{2P_c}\sum_{p=-\infty}^{\infty}\sum_{q=-\infty}^{\infty} a_{p,q}\cdot e^{j(\varphi_c(t)+p\varphi_d(t)+q\varphi_l(t))} \tag{A7}$$

$\mathbf{M}_C[\bullet]$ generally represents the response function of MOD_C and depends on the modulation scheme such as intensity modulation, phase modulation, and frequency modulation [7]. $a_{p,q}$ is given as the two-dimensional Fourier coefficient as a function of V_d and V_l. An optical SSB filter that follows extracts, for example, only the optical carrier and first-order LSBs, as shown in Fig. 9(b). The complex electric field of optical SSB signal $e_2(t)$ is then expressed as

$$e_2(t) \propto \sqrt{2P_c}\Big[a_{-1,0}\cdot e^{j\{\varphi_c(t)-\varphi_d(t)\}} + a_{0,-1}\cdot e^{j\{\varphi_c(t)-\varphi_l(t)\}} + a_{0,0}\cdot e^{j\varphi_c(t)}\Big]. \tag{A8}$$

This is transmitted to a remote BS as an optical downlink signal.

After transmitted over a downlink optical fiber with the length of L_d and the propagation constant of $\beta_d(f)$, the optical downlink signal is split by an optical power divider. It is assumed that the propagation loss of the downlink optical fiber is compensated by optical amplifiers. One part of the optical downlink signal is used to regenerate the RF downlink signal in the BS, the other part is used to transmit an RF uplink signal. The complex electric fields of former and later optical signals $e_{2d}(t, L_d)$ and $e_{2u}(t, L_d)$ are then written as

$$\begin{aligned} e_{2d}(t, L_d) &= \sqrt{\alpha_{\mathrm{opd}}}\cdot e_2(t)\cdot\exp\{-j\beta_d(f)\cdot L_d\} \\ &\propto \sqrt{2\alpha_{\mathrm{opd}}P_c}\times\Big[a_{-1,0}\cdot e^{j\psi_{-1,0}(t,L_d)} + a_{0,-1}\cdot e^{j\psi_{0,-1}(t,L_d)} + a_{0,0}\cdot e^{j\psi_{0,0}(t,L_d)}\Big] \end{aligned} \tag{A9}$$

$$\begin{aligned} e_{2u}(t, L_d) &= \sqrt{(1-\alpha_{\mathrm{opd}})}e_2(t)\cdot\exp\{-j\beta_d(f)\cdot L_d\} \\ &\propto \sqrt{2(1-\alpha_{\mathrm{opd}})P_c}\times\Big[a_{-1,0}\cdot e^{j\psi_{-1,0}(t,L_d)} + a_{0,-1}\cdot e^{j\psi_{0,-1}(t,L_d)} + a_{0,0}\cdot e^{j\psi_{0,0}(t,L_d)}\Big] \end{aligned} \tag{A10}$$

where $\psi_{p,q}(t, L_d)$ is defined as

$$\begin{aligned} \psi_{p,q}(t, L_d) &\equiv \varphi_c(t) + p\varphi_d(t) + q\varphi_l(t) - \beta_d(f)\cdot L_d \\ &\simeq 2\pi(f_c + pf_d + qf_l)(t-\beta_{d1}L_d) + \phi_c(t-\beta_{d1}L_d) + p\theta_d(t-\beta_{d1}L_d) \\ &\quad - \frac{1}{2}\beta_{d2}\cdot\{2\pi(pf_d+qf_l)\}^2\cdot L_d - (\beta_{d0}-\beta_{d1}\cdot 2\pi f_c)\cdot L_d. \end{aligned} \tag{A11}$$

Here, α_{opd} is the bifurcation ratio of the optical power divider, the propagation constant $\beta_d(f)$ is approximated as [13]

$$\beta_d(f) \simeq \beta_{d0} + \beta_{d1}\cdot 2\pi(f-f_c) + \frac{1}{2}\beta_{d2}\cdot\{2\pi(f-f_c)\}^2. \tag{A12}$$

Here, $\beta_{d1}L_d$ corresponds to the group-delay time, and β_{d2} is related with the dispersion of downlink fiber D_d as

$$\beta_{d2} = -\frac{\lambda^2}{2\pi c}\cdot D_d. \tag{A13}$$

λ and c are the wavelength in the fiber and the velocity in the vacuum, respectively. By using the photodetector (PD_B) in the BS, three interest photocurrents are generated from the optical downlink signal $e_{2d}(t, L_d)$ as shown in Fig. 9(c).

$$i_{c,d}(t, L_d) = 2\mathcal{R}_B\alpha_{\mathrm{opd}}P_c \cdot a_{0,0}a_{-1,0} \cdot \exp\{j\varphi_{c,d}(t, L_d)\} \tag{A14}$$

$$i_{c,l}(t, L_d) = 2\mathcal{R}_B\alpha_{\mathrm{opd}}P_c \cdot a_{0,0}a_{0,-1} \cdot \exp\{j\varphi_{c,l}(t, L_d)\} \tag{A15}$$

$$i_{d,l}(t, L_d) = 2\mathcal{R}_B\alpha_{\mathrm{opd}}P_c \cdot a_{-1,0}a_{0,-1} \cdot \exp\{j\varphi_{l,d}(t, L_d)\}. \tag{A16}$$

In the above equations, $\mathcal{R}_B$ is the responsivity of PD_B and then $\varphi_{c,d}(t, L_d)$, $\varphi_{c,l}(t, L_d)$, and $\varphi_{l,d}(t, L_d)$ are, respectively, given as

$$\begin{aligned}\varphi_{c,d}(t, L_d) &= \psi_{0,0}(t, L_d) - \psi_{-1,0}(t, L_d)\\ &= 2\pi f_d(t - \beta_{d1}L_d) + \theta_d(t - \beta_{d1}L_d)\\ &\quad - \frac{1}{2}\beta_{d2}(2\pi f_d)^2 L_d,\end{aligned} \tag{A17}$$

$$\begin{aligned}\varphi_{c,l}(t, L_d) &= \psi_{0,0}(t, L_d) - \psi_{0,-1}(t, L_d)\\ &= 2\pi f_l(t - \beta_{d1}L_d) - \frac{1}{2}\beta_{d2}(2\pi f_l)^2 L_d\end{aligned} \tag{A18}$$

$$\begin{aligned}\varphi_{l,d}(t, L_d) &= \psi_{0,-1}(t, L_d) - \psi_{-1,0}(t, L_d)\\ &= 2\pi(f_d - f_l)(t - \beta_{d1}L_d)\\ &\quad + \theta_d(t - \beta_{d1}L_d) - \frac{1}{2}\beta_{d2}(2\pi f_d)^2 L_d\\ &\quad + \frac{1}{2}\beta_{d2}(2\pi f_l)^2 L_d.\end{aligned} \tag{A19}$$

We neglect the dispersion effect due to both the laser phase noise $\phi_c(t)$ and the downlink data $\theta_d(t)$ because they do not seriously influence the system performance in actual fiber-optic access networks with standard SMFs. For example, the linewidth of laser will be several 10 MHz at most, the maximum data rate of the RF signal will be several 100 Mb/s, the total fiber length will be $\leq$ several tens of kilometers, and the fiber dispersion will be typically 17 ps/nm/km. In this case, since the maximum difference of group delay will be 1 ps at most, it is trivial for the several hundred megabit-per-second data Only the desired downlink RF signal $i_{c,d}(t, L_d)$ is then selected out by an electrical BPF ($\mathrm{e-BPF}_B$) and propagated via a millimeter-wave antenna to a terminal. Note that in (A17), the last term is a constant phase, and there is no laser phase noise term. If the payload data of the RF downlink signal $\theta_d(t)$ is deferentially encoded and the propagating RF downlink signal $i_{c,d}(t, L_d)$ is then demodulated by the differential detection, the data for the downlink can be extracted without any fiber dispersion effect, as well as no laser phase noise.

The other fraction of the optical downlink signal ($e_{2u}(t, L_d)$) is modulated with the RF uplink signal $m_u(t)$ by another optical modulator (MOD_B) in the BS.

$$m_u(t) = V_u \exp\{j\varphi_u(t)\} \tag{A20}$$

$$\varphi_u(t) = 2\pi f_u t + \theta_u(t). \tag{A21}$$

V_u, f_u, and $\theta_u(t)$ are the amplitude, the carrier frequency, and the payload data of the RF uplink signal, respectively. The complex electric field of the modulated optical signal $e_3(t, L_d)$ is then written by

$$\begin{aligned}e_3(t, L_d) &= \mathbf{M}_B[m_u(t)] \cdot e_{2u}(t, L_d)\\ &\propto \sqrt{2(1-\alpha_{\mathrm{opd}})P_c} \cdot a_{-1,0}\\ &\quad \cdot \sum_{r=-\infty}^{\infty} b_r \cdot e^{j(\psi_{-1,0}(t) + r\varphi_u(t))}\\ &\quad + \sqrt{2(1-\alpha_{\mathrm{opd}})P_c} \cdot a_{0,-1}\\ &\quad \cdot \sum_{r=-\infty}^{\infty} b_r \cdot e^{j(\psi_{0,-1}(t) + r\varphi_u(t))}\\ &\quad + \sqrt{2(1-\alpha_{\mathrm{opd}})P_c} \cdot a_{0,0}\\ &\quad \cdot \sum_{r=-\infty}^{\infty} b_r \cdot e^{j(\psi_{0,0}(t) + r\varphi_u(t))}\end{aligned} \tag{A22}$$

where $\mathbf{M}_B[\bullet]$ represents the response function of MOD_B and also depends on the modulation schemes. b_r is given as the Fourier coefficient as a function of V_u. Another optical narrow BPF ($\mathrm{o-BPF}_B$) in the BS extracts one set of the first-order LSB from $e_3(t, L_d)$, as shown in Fig. 9(e). The resultant is looped back to the CS, called optical uplink signal. The complex electric field of optical uplink signal $e_4(t, L_d)$ is written as

$$\begin{aligned}&e_4(t, L_d)\\ &\quad \propto \sqrt{2(1-\alpha_{\mathrm{opd}})P_c} \times \Big[a_{-1,0} \cdot b_0 \cdot e^{j\psi_{-1,0}(t, L_d)}\\ &\qquad + a_{0,-1} \cdot b_0 \cdot e^{j\psi_{0,-1}(t, L_d)}\\ &\qquad + a_{0,0} \cdot b_{-1}\\ &\qquad \cdot e^{j\{\psi_{0,0}(t, L_d) - \varphi_u(t)\}}\Big].\end{aligned} \tag{A23}$$

The optical uplink signal returns to the CS over an uplink optical fiber with the length of L_u and propagation constant of $\beta_u(f)$. It is also assumed that the propagation loss of the uplink optical fiber is compensated by optical amplifiers. The complex electric fields of the optical uplink signal $e_{4u}(t, L_d, L_u)$ is then rewritten as

$$\begin{aligned}e_{4u}(t, L_d, L_u) &= e_4(t, L_d) \cdot \exp\{-j\beta_u(f) \cdot L_u\}\\ &= \sqrt{2(1-\alpha_{\mathrm{opd}})P_c}\\ &\quad \times \Big[a_{-1,0} \cdot b_0 \cdot e^{j\upsilon_{-1,0,0}(t, L_d, L_u)}\\ &\qquad + a_{0,-1} \cdot b_0 \cdot e^{j\upsilon_{0,-1,0}(t, L_d, L_u)}\\ &\qquad + a_{0,0} \cdot b_{-1} \cdot e^{j\upsilon_{0,0,-1}(t, L_d, L_u)}\Big]\end{aligned} \tag{A24}$$

where $\upsilon_{p,q,r}(t, L_d, L_u)$ is defined as

$$\begin{aligned}\upsilon_{p,q,r}(t, L_d, L_u) &\equiv \varphi_c(t) + p\varphi_d(t) + q\varphi_l(t) - \beta_d(f)\cdot L_d - \beta_u(f)\cdot L_u \\ &\simeq 2\pi(f_c + pf_d + qf_l + rf_u)\cdot(t - \beta_{d1}L_d - \beta_{u1}L_u) \\ &\quad + \phi_c(t - \beta_{d1}L_d - \beta_{u1}L_u) + p\theta_d(t - \beta_{d1}L_d - \beta_{u1}L_u) \\ &\quad + r\theta_u(t - \beta_{u1}L_u) - \frac{1}{2}\beta_{d2}\cdot\left\{2\pi(pf_d + qf_l)\right\}^2\cdot L_d \\ &\quad - \frac{1}{2}\beta_{u2}\cdot\left\{2\pi(pf_d + qf_l + rf_u)\right\}^2\cdot L_u \\ &\quad - \left\{\beta_{d0} - \beta_{d1}\cdot 2\pi(f_c + rf_u)\right\}\cdot L_d \\ &\quad - \left\{\beta_{u0} - \beta_{u1}\cdot 2\pi f_c\right\}\cdot L_u. \end{aligned} \tag{A25}$$

Again, the propagation constant $\beta_u(f)$ is approximated as

$$\beta_u(f) \simeq \beta_{u0} + \beta_{u1}\cdot 2\pi(f - f_c) + \frac{1}{2}\beta_{u2}\cdot\left\{2\pi(f - f_c)\right\}^2. \tag{A26}$$

Here, $\beta_{u1}L_u$ corresponds to the group-delay time and β_{u2} is related with the dispersion of downlink fiber D_u as

$$\beta_{u2} = -\frac{\lambda^2}{2\pi c}\cdot D_u. \tag{A27}$$

By using the photodetector (PD_C) in the CS, three interest photocurrents are generated from the optical downlink signal $e_{4u}(t, L_d, L_u)$, as shown in Fig. 9(f).

$$i_{l,u}(t, L_d, L_u) = 2\mathcal{R}_C(1 - \alpha_{\mathrm{opd}})P_c\cdot a_{0,0}a_{0,-1}b_0b_{-1}\cdot e^{j\varphi_{l,u}(t, L_d, L_u)} \tag{A28}$$

$$i_{l.d}(t, L_d, L_u) = 2\mathcal{R}_C(1 - \alpha_{\mathrm{opd}})P_c\cdot a_{-1,0}a_{0,-1}b_0^2\cdot e^{j\varphi_{l,d}(t, L_d, L_u)} \tag{A29}$$

$$i_{d,u}(t, L_d, L - u) = 2\mathcal{R}_C(1 - \alpha_{\mathrm{opd}})P_c\cdot a_{0,0}a_{-1,0}b_0b_{-1}\cdot e^{j\varphi_{d,u}(t, L_d, L_u)}. \tag{A30}$$

In the above equations, $\mathcal{R}_C$ is the responsivity of PD_C, and $\varphi_{l,d}(t, L_d, L_u)$, $\varphi_{l,u}(t, L_d, L_u)$, and $\varphi_{u,d}(t, L_d, L_u)$ are, respectively, given as

$$\begin{aligned}\varphi_{l,u}(t, L_d, L_u) &= \upsilon_{0,-1,0}(t, L_d, L_u) - \upsilon_{0,0,-1}(t, L_d, L_u) \\ &= 2\pi(f_u - f_l)(t - \beta_{d1}L_d - \beta_{u1}L_u) + \theta_u(t - \beta_{u1}L_u) \\ &\quad - \frac{1}{2}\beta_{d2}(2\pi f_l)^2L_d - \frac{1}{2}\beta_{u2}(2\pi f_l)^2L_u \\ &\quad + \frac{1}{2}\beta_{u2}(2\pi f_u)^2L_u + \beta_{d1}(2\pi f_u)L_d \end{aligned} \tag{A31}$$

$$\begin{aligned}\varphi_{l,d}(t, L_d, L_u) &= \upsilon_{0,-1,0}(t, L_d, L_u) - \upsilon_{-1,0,0}(t, L_d, L_u) \\ &= 2\pi(f_d - f_l)(t - \beta_{d1}L_d - \beta_{u1}L_u) \\ &\quad + \theta_d(t - \beta_{d1}L_d - \beta_{u1}L_u) \\ &\quad - \frac{1}{2}\beta_{d2}(2\pi f_l)^2L_d - \frac{1}{2}\beta_{u2}(2\pi f_l)^2L_u \\ &\quad + \frac{1}{2}\beta_{d2}(2\pi f_d)^2L_d + \frac{1}{2}\beta_{u2}(2\pi f_d)^2L_u \end{aligned} \tag{A32}$$

$$\begin{aligned}\varphi_{d,u}(t, L_d, L_u) &= \upsilon_{-1,0,0}(t, L_d, L_u) - \upsilon_{0,0,-1}(t, L_d, L_u) \\ &= 2\pi(f_u - f_d)(t - \beta_{d1}L_d - \beta_{u1}L_u) \\ &\quad + \theta_u(t - \beta_{u1}L_u) - \theta_d(t - \beta_{d1}L_d - \beta_{u1}L_u) \\ &\quad - \frac{1}{2}\beta_{d2}(2\pi f_d)^2L_d - \frac{1}{2}\beta_{u2}(2\pi f_d)^2L_u \\ &\quad + \frac{1}{2}\beta_{u2}(2\pi f_u)^2L_u + \beta_{d1}(2\pi f_u)L_d. \end{aligned} \tag{A33}$$

The photodetected signal are directly downconverted in the IF band by the photonic downconversion [7]. We neglect the dispersion effect due to the uplink data $\theta_d(t)$, Only the desired uplink IF signal $i_{l,u}(t, L_d, L_u)$ is then selected out by another electrical BPF ($\mathrm{e-BPF}_C$) and put into a following IF demodulator to extract the payload data for the uplink. Note that in (A31), the last four terms are constant phases, and there is no laser phase-noise term. If the payload data of the RF uplink signal $\theta_u(t)$ is deferentially encoded and then the downconverted IF downlink signal $i_{l,u}(t, L_d, L_u)$ is demodulated by the differential detection, the data for the uplink can also be extracted without any fiber dispersion effect, as well as no laser phase noise.

ACKNOWLEDGMENT

The authors wish to thank T. Ushikubo, Oki Electric Industry Company Ltd., Kanagawa, Japan, for collaborating in this experiment. Author T. Kuri also thanks N. Otani, T. Itabe, and T. Iida, all of the Communications Research Laboratory, Tokyo, Japan, for their encouragement.

REFERENCES

[1] T. Tanuma, "Current frequency management and utilization of millimeter-wave band in Japan," in *Topical Millimeter Waves Symp. Technical Dig.*, Yokosuka, Japan, Mar. 2000, Session 2-1, pp. 11–14.

[2] S. Ohmori, "Toward future wireless multimedia communication systems using millimeter-waves," in *IEEE Int. Microwave Photonics Topical Meeting Technical Dig.*, Melbourne, Australia, Nov. 1999, Paper W-1.1, p. 3.

[3] F. Deborgies, M. Mittrich, H. Schmuck, P. Jaffre, and C. Pescod, "Progress in the ACTS FRANS project," in *IEEE Int. Microwave Photonics Topical Meeting Technical Dig.*, Melbourne, Australia, Nov. 1999, Paper T-7.1, pp. 115–118.

[4] A. Nirmalathas, C. Lim, D. Novak, and R. Waterhouse, "Optical interface without light sources for base-station designs in fiber-wireless systems incorporating WDM," in *IEEE Int. Microwave Photonics Topical Meeting Technical Dig.*, Melbourne, Australia, Nov. 1999, Paper T-7.2, pp. 119–122.

[5] K. Kitayama, "Architectural considerations of fiber-radio millimeter-wave wireless access systems," *Fiber Integr. Opt.*, vol. 19, pp. 167–186, 2000.

[6] T. Kuri, K. Kitayama, A. Stöhr, and Y. Ogawa, "Fiber-optic millimeter-wave downlink system using 60-GHz-band external modulation," *J. Lightwave Technol.*, vol. 17, pp. 799–806, May 1999.
[7] T. Kuri, K. Kitayama, and Y. Ogawa, "Fiber-optic millimeter-wave uplink system incorporating remotely fed 60-GHz-band optical pilot tone," *IEEE Trans. Microwave Theory Tech.*, vol. 47, pp. 1332–1337, July 1999.
[8] L. Noël, D. Wake, D. G. Moodie, D. D. Marcenac, L. D. Westbrook, and D. Nesset, "Novel Techniques for high-capacity 60-GHz fiber-radio transmission systems," *IEEE Trans. Microwave Theory Tech.*, vol. 45, pp. 1416–1423, Aug. 1997.
[9] T. Kuri, K. Kitayama, and Y. Takahashi, "Simplified BS without light source and RF local oscillator in full-duplex millimeter-wave radio-on-fiber system based upon external modulation technique," in *IEEE Int. Microwave Photonics Topical Meeting Technical Dig.*, 1999, Paper T-7.3, pp. 123–126.
[10] F. Devaux, U. Sorel, and J. F. Kerdiles, "Simple measurement of fiber dispersion and of chirp parameter of intensity modulated light emitter," *J. Lightwave Technol.*, vol. 11, pp. 1937–1940, Dec. 1993.
[11] T. Kuri and K. Kitayama, "Long-term stabilized millimeter-wave generation using a high-power and mode-locked laser diode module," *IEEE Trans. Microwave Theory Tech.*, vol. 47, pp. 570–574, May 1999.
[12] J. Park, W. V. Sorin, and K. Y. Lau, "Elimination of the fiber chromatic dispersion penalty on 1550 nm millimeter-wave optical transmission," *Electron. Lett.*, vol. 33, no. 6, pp. 512–513, Mar. 1997.
[13] G. P. Agrawal, *Nonlinear Optics*, 2nd ed. New York: Academic, 1995, sec. 2 to 4.
[14] T. Kuri, K. Kitayama, and K. Murashima, "Error-free DWDM transmission of 60-GHz-band fiber-radio signals with square-like response fiber Bragg gratings," in *IEEE Int. Microwave Photonics Topical Meeting Technical Dig.*, Jan. 2001, Paper Tu.2-6, pp. 69–72.

Toshiaki Kuri (S'93–M'96) received the B.E., M.E., and Ph.D. degrees from Osaka University, Osaka, Japan, in 1992, 1994, and 1996, respectively.

In 1996, he joined the Communications Research Laboratory (CRL), Ministry of Posts and Telecommunications (now the Independent Administrative Institution), Tokyo, Japan, where he is mainly engaging in research on optical communication systems.

Dr. Kuri is a member of the Institute of Electrical, Information and Communication Engineers (IEICE), Japan. He was the recipient of the 1998 Young Engineer Award presented by the IEICE.

Ken-ichi Kitayama (S'75–M'76–SM'89) received the B.E., M.E., and Dr.Eng. degrees in communication engineering from Osaka University, Osaka, Japan, in 1974, 1976, and 1981, respectively.

In 1976, he joined the NTT Electrical Communication Laboratory. From 1982 to 1983, he was a Visiting Scholar with the University of California at Berkeley. In 1995, he joined the Communications Research Laboratory, Ministry of Posts and Telecommunications, Tokyo, Japan. Since 1999, he has been with Osaka University, where he is currently a Professor. He has authored over 160 papers in refereed journals. He holds over 30 patents. His research interests are photonic networks and fiber-optic wireless communications.

Prof. Kitayama is a member of the Institute of Electrical, Information and Communication Engineers (IEICE), Japan, the Japan Society of Applied Physics, and the Optical Society of America (OSA). He serves on the Editorial Boards of the IEEE PHOTONICS TECHNOLOGY LETTERS and the IEEE TRANSACTIONS ON COMMUNICATIONS. He was the recipient of the 1980 Young Engineer Award presented by the IEICE and the 1985 Paper Award of Optics presented by the Japan Society of Applied Physics.

Yoshiro Takahashi was born in Tokyo, Japan, in 1957. He received the B.S. and M.S. degrees in electrical engineering from Nihon University, Tokyo, Japan, in 1980 and 1982 respectively.

In April 1982, he joined the Oki Electric Industry Company Ltd., where he was involved with the development of microelectronics technology. From 1982 to 1998, he was engaged in the development of LED electrophotographic printing engines, copper–polyimide thin-film multilayer (TFML) 2.4-Gb/s exchange modules, and high-density interconnection technology that used the surface laminar printed wiring board (PWB). His current activities concern the area of high-frequency/high-speed subsystems, especially millimeter-wave band subsystems.